

Received 20xx month day; accepted 20xx month day

Galaxy interactions in filaments and sheets: insights from EAGLE simulations

Apashanka Das¹, Biswajit Pandey² and Suman Sarkar³

¹ Department of Physics, Visva-Bharati University, Santiniketan, Birbhum, 731235, India
a.das.cosmo@gmail.com

² Department of Physics, Visva-Bharati University, Santiniketan, Birbhum, 731235, India
biswap@visva-bharati.ac.in

³ Department of Physics, Indian Institute of Technology, Kharagpur, 721302, India
suman2reach@gmail.com

Abstract We study the colour and star formation rates of paired galaxies in filaments and sheets using the EAGLE simulations. We find that the major pairs with pair separation < 50 kpc are bluer and more star forming in filamentary environments compared to those hosted in sheet-like environments. This trend reverses beyond a pair separation of ~ 50 kpc. The interacting pairs with larger separations (> 50 kpc) in filaments are on average redder and low-star forming when compared to those embedded in sheets. The galaxies in filaments and sheets may have different stellar mass and cold gas mass distributions. Using a KS test, we find that for paired galaxies with pair separation < 50 kpc, there are no significant differences in these properties in sheets and filaments. The filaments transport gas towards the cluster of galaxies. Some earlier studies find preferential alignment of galaxy pairs with filament axis. Such alignment of galaxy pairs may lead to different gas accretion efficiency in galaxies residing in filaments and sheets. We propose that the enhancement of star formation rate at smaller pair separation in filaments is caused by the alignment of galaxy pairs. A recent study with the SDSS data (Das, Pandey & Sarkar 2023) reports the same findings. The confirmation of these results by the EAGLE simulations suggests that the hydrodynamical simulations are powerful theoretical tools for studying the galaxy formation and evolution in the cosmic web.

Key words: methods: data analysis — statistical — galaxies: interactions — evolution — cosmology: large scale structure of the universe

1 INTRODUCTION

Understanding the formation and evolution of galaxies is one of the most challenging problems in cosmology. The formation and evolution of galaxies are expected to be influenced by both the initial conditions at the location of their formation and their interactions with the surrounding environment. The primordial density perturbations in the dark matter density field grow due to gravitational instability and eventually collapse into dark matter halos. The dark matter halos represent the peaks in the density field. The halos are surrounded by diffuse neutral Hydrogen distribution after the recombination. They accrete the gas which radiate away their kinetic energy and settle down at their centers. The cooling and condensation of the gas at the centre of the dark matter halos are believed to be the primary mechanism for

the formation of galaxies (Rees & Ostriker 1977; Silk 1977; White & Rees 1978; Fall & Efstathiou 1980).

The galaxies interact with other galaxies and their environments. The galaxy-galaxy interactions are known to enhance the star formation activity in galaxies (Barton, Geller & Kenyon 2000; Lambas et al. 2008; Alonso et al. 2004; Nikolic, Cullen & Alexander 2004; Alonso et al. 2006; Woods, Geller & Barton 2006; Woods & Geller 2007; Barton et al. 2007; Ellison et al. 2008; Heiderman et al. 2009; Knapen & James 2009; Robaina et al. 2009; Ellison et al. 2010; Woods et al. 2010; ?). The environment of a galaxy plays a decisive role in its evolution. The galaxies in high density regions are redder and have lower star formation rates (Lewis et al. 2002; Gómez et al. 2003; Kauffmann et al. 2004). The suppression of star formation in high density regions may occur due to different physical mechanisms. Some of the known physical mechanisms are ram pressure stripping (Gunn & Gott 1972), galaxy harassment (Moore et al. 1996; Moore, Lake & Katz 1998), strangulation (Gunn & Gott 1972; Balogh, Navarro & Morris 2000), starvation (Larson, Tinsley & Caldwell 1980; Somerville & Primack 1999; Kawata & Mulchaey 2008) and gas loss through starburst, AGN or shock-driven winds (Cox et al. 2004; Murray, Quataert & Thompson 2005; Springel, Matteo & Hernquist 2005). A number of other physical processes such as mass quenching (Birnboim & Dekel 2003; Dekel & Birnboim 2006; Kereš et al. 2005; Gabor et al. 2010), morphological quenching (Martig et al. 2009), bar quenching (Masters et al. 2010) and angular momentum quenching (Peng & Renzini 2020) can also halt star formation in galaxies.

The environmental dependence of galaxy properties remains an active area of research for the last few decades. The galaxy properties are known to strongly depend on environment (Oemler 1974; Davis & Geller 1976; Dressler 1980; Guzzo et al. 1997; Zehavi et al. 2002; Hogg et al. 2003; Blanton et al. 2003; Einasto et al. 2003; Goto et al. 2003; Kauffmann et al. 2004; Pandey & Bharadwaj 2006; Park et al. 2007; Mouhcine, Baldry & Bamford 2007; Pandey & Bharadwaj 2008; Porter et al. 2008; Bamford, Nichol & Baldry 2009; ?; Koyama et al. 2013; Pandey & Sarkar 2017; Sarkar & Pandey 2020; Bhattacharjee, Pandey & Sarkar 2020; Pandey & Sarkar 2020). Most of the studies on the environmental dependence of galaxy properties treat the local density as a proxy for the environment. The local density undoubtedly plays a decisive role in galaxy evolution. However, the local density alone can not characterize the environment of a galaxy. The observations from different redshift surveys (Gregory & Thompson 1978; Joeveer & Einasto 1978; Einasto, Joeveer, & Saar 1980; Zeldovich & Shandarin 1982; Einasto et al. 1984; Bharadwaj et al. 2000; Pandey & Bharadwaj 2005) indicate that galaxies are distributed in an interconnected network-like pattern of clusters, filaments and sheets surrounded by vast empty regions. This network is often referred to as the “cosmic web” (Bond, Kofman & Pogosyan 1996). The galaxies and their host halos are embedded in different geometric environments of the cosmic web. Pandey & Bharadwaj (2008) find that the star forming blue galaxies have a more filamentary distribution compared to the red galaxies. A number of studies with hydrodynamical simulations suggest that 80% of the baryonic budget in the Universe is accounted by low density gas (WHIM) in filaments (Tuominen 2021; Galarraga-Espinosa et al. 2021). Consequently, the gas accretion efficiency in the dark matter halos in filaments and sheets may differ in a significant manner. Thus, cosmic web can have significant impact on the properties and evolution of galaxies. The galaxies that are located in different parts of the cosmic web can experience different physical conditions, such as different densities of gas, different levels of tidal forces, different frequency of interactions and mergers. All these factors may play important roles in shaping the properties and evolution of galaxies.

The interactions between galaxies with comparable masses are known as the major interactions. Such interactions are known to trigger new star formation in galaxies. The interacting pairs are expected to be present in different geometric environments of the cosmic web. They are more frequently observed in the denser regions of the cosmic web. The filaments and sheets, being the denser parts of the cosmic web, host a significant number of major galaxy pairs. In a recent work, Das, Pandey & Sarkar (2023) analyze the SDSS data to compare the star formation rate and colour of major pairs hosted in filaments and sheets. They find that the major galaxy pairs with separation < 50 kpc are relatively high star forming and bluer when hosted in filaments. On the other hand, the major pairs with separation > 50 kpc

show a significantly higher SFR and colour in sheet-like environments. This behaviour may be related to the preferential alignment of galaxy pairs with the filament axis (Tempel & Tamm 2015; Mesa et al. 2018). The available gas mass is a primary regulator of the star formation in a galaxy. The gas mass is modulated by the inflows and outflows (Dekel, Sari, & Coverino 2009; Davé, Finlator, & Oppenheimer 2011; Davé, Finlator, & Oppenheimer 2012; Lilly et al. 2013). The transient events like interactions and mergers can drive the galaxies out of equilibrium. The alignment of galaxy pairs with filament spines may lead to anisotropic accretion and higher gas accretion efficiency in these galaxies. The primary aim of this work is to verify these findings with hydrodynamical simulation.

The EAGLE simulation (McAlpine et al. 2016) is a hydrodynamical simulation that studies the galaxy formation and evolution in a cosmological volume. It describes the formation of large-scale structures as well as the formation of galaxies by gas falling into the dark matter halos and their subsequent cooling and condensation. It would be interesting to study the SFR and colour of the major pairs in filaments and sheets using EAGLE simulations. In observations, the galaxy pairs are usually identified by employing simultaneous cuts on the projected separation and the rest frame velocity difference of the galaxies. However, all these pairs may not be undergoing interactions. Some of the pairs identified in observations may not be close in three dimensions due to the chance superposition in the high-density regions like groups and clusters (Alonso et al. 2004). Also, we can not construct a mock catalogue for the observational sample of galaxy pairs used in Das, Pandey & Sarkar (2023) due to the smaller volume of the EAGLE simulations. So we decided to use the real-space positions of galaxies available in simulation to identify the major pairs. This would avoid any errors in identification of galaxy pairs due to the projection effects. We identify the geometric environments of galaxy pairs using the local dimension (Sarkar & Bharadwaj 2009). Our primary aim of this work is to study the interaction induced star formation in filaments and sheets using EAGLE simulations. This would help us to assess the roles of the large-scale structures like filaments and sheets in galaxy evolution.

We organize the paper as follows: we describe the data and the method of analysis in Section 2 and present the results and conclusions in Section 3.

2 DATA AND METHOD OF ANALYSIS

2.1 EAGLE simulation data

The EAGLE simulation (McAlpine et al. 2016) is a set of cosmological hydrodynamical simulation in periodic, cubic comoving volumes ranging from side of length 25 to 100 megaparsec that track the evolution of both baryonic (gas, stars and massive black holes) and non-baryonic (dark matter) elements from a starting redshift of $z = 127$ to the present day. This simulation adopts a flat Λ CDM cosmology with parameters taken from the *Planck* mission results (Planck Collaboration et al. 2014). The values of cosmological parameters used in this simulation are $\Omega_\Lambda = 0.693$, $\Omega_m = 0.307$, $\Omega_b = 0.04825$ and $H_0 = 67.77$ km/s/Mpc, where symbols have their usual meanings.

We download the various properties of galaxies from the publicly available EAGLE run simulation using *wget* command. We extract the information of position of the centre of mass of galaxies in three dimension within a comoving cubic volume of size 100 Mpc^3 from *Ref - L0100N1504_Subhalo* table. We consider the last snapshot of the simulation having *Snapshot* = 28 which corresponds to redshift $z = 0$. We select only those galaxies which are flagged as *Spurious* = 0. This ensures that we select only the genuine simulated galaxies by discarding all the unusual objects with very small stellar mass and anomalously high metallicity or black hole mass. We also download the star formation rate, stellar mass and cold gas mass of simulated galaxies using *Ref - L0100N1504_Aperture* table. These are estimated within a spherical 3D aperture of radius 30 physical kpc centered at the location of minimum gravitational potential of a galaxy. Use of this criteria gives well suited stellar mass and star formation estimates as compared to observational results and is also recommended for use by the EAGLE simulation team (McAlpine et al. 2016). We also consider only those galaxies with their stellar mass > 0 . Combining the two tables with *GalaxyID*, we obtain all of the above mentioned information for 325358 galaxies. We also extract the non-dust attenuated rest frame broad band magnitudes

Local dimension	Geometric environment
$0.75 \leq D < 1.25$	$D1$
$1.25 \leq D < 1.75$	$D1.5$
$1.75 \leq D < 2.25$	$D2$
$2.25 \leq D < 2.75$	$D2.5$
$D \geq 2.75$	$D3$

Table 1: This table shows range of local dimension values D and the associated geometric environment of galaxies.

of galaxies estimated in u and r band filters (Doi et al. 2010) from *Ref - L0100N1504_Magnitude* table, where u and r respectively denote Ultraviolet and Red filter bands of Sloan Digital Sky Survey (SDSS). We combine this table with *Ref - L0100N1504_Subhalo* and *Ref - L0100N1504_Aperture* table using *GalaxyID* to get all the required information. The magnitude of galaxies in different SDSS filters have been computed in 30 physical kpc spherical apertures following the procedure described in Trayford et al. (2015). Finally, we have all the information for 29754 galaxies. For the rest of the analysis, we refer to $u - r$ colour of galaxies as the difference of its rest frame non-dust attenuated absolute magnitudes in u and r band respectively. Only the magnitudes of the galaxies with stellar mass $\log(M_{\text{stellar}}/M_{\text{sun}}) > 10^{8.5}$ are provided in *Ref - L0100N1504_Subhalo* table. However, here we use the stellar mass estimates of galaxies from *Ref - L0100N1504_Aperture* table where the minimum stellar mass of a galaxy is $\log(M_{\text{stellar}}/M_{\text{sun}}) \sim 10^{8.2}$. Observations show that the galaxies with stellar mass $M_{\text{stellar}} < 3 \times 10^{10} M_{\text{sun}}$ are actively star forming and the galaxies having stellar masses above this critical value are generally quiescent systems (Kauffmann et al. 2003). For the present analysis, we consider only those galaxies which have their stellar mass in between $8.5 \leq \log(M_{\text{stellar}}/M_{\text{sun}}) \leq 10.5$. Our mass limited sample contains a total 21305 galaxies.

We identify the nearest neighbour in three dimensions for each galaxy in our mass limited sample. The distance to the nearest neighbour for each galaxy is denoted by r , where r represents the three dimensional distance between the centre of mass of the galaxies. Initially, we label each galaxy and its nearest neighbour in our sample as a possible pair. We then select only those pairs for which $r \leq 200$ kpc. We also apply a cut on their stellar mass ratio $1 \leq \frac{M_1}{M_2} < 3$ to include only the major pairs in our analysis. This provides us with a total 2264 major pairs. The smallest pair separation in our sample is ~ 6 kpc.

We quantify the geometric environment of the galaxies in the EAGLE simulation by estimating their local dimension on a length scale of 10 Mpc (subsection 2.2). We use *GalaxyID* to cross match these galaxies with our pair sample. The cross-matching yields a total 2537 galaxies in major pairs. We find that 373 and 276 out of these galaxies are residing in filaments and sheets respectively. It may be noted that the local dimension can not be determined for all the galaxies in the simulation.

2.2 Morphology of the local environment

We characterize the different geometric environments of the cosmic web using the local dimension (Sarkar & Bharadwaj 2009). The local dimension is a simple measure based on the number counts of galaxies within spheres of different radii centered on a galaxy. The number counts of galaxies within a sphere of radius R centered on a galaxy can be written as,

$$N(< R) = A R^D \quad (1)$$

where A is a constant and D is the local dimension. The number counts $N(< R)$ would scale differently with the radius R depending on the local geometry of the embedding environment. We vary the radius of the measuring sphere between $R_1 \text{ Mpc} \leq R \leq R_2 \text{ Mpc}$ and consider only those galaxies for which at least 10 galaxies are available within this range. We fit the observed number counts $N(< R)$ to Equation 1 and determine the best fit values of A and D using a least-square fitting. The goodness of each fit is determined by estimating the χ^2 per degree of freedom. Only the fits with chi-square

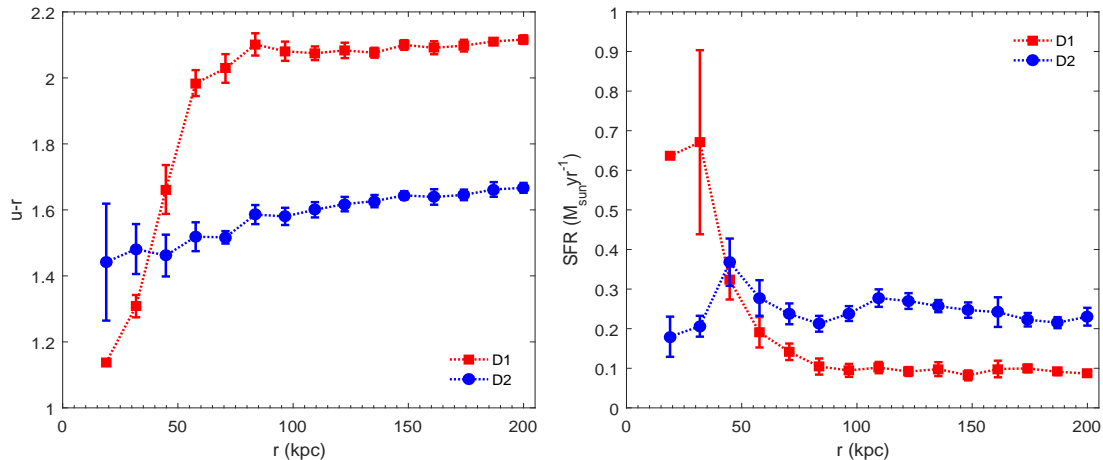


Fig. 1: The plot in the left and right panel respectively shows cumulative mean $u - r$ colour and SFR of major pairs as a function of pair separation r . The 1σ error bars at each data point shown are obtained using 10 Jackknife samples.

per degree of freedom $\frac{\chi^2}{\nu} \leq 0.5$ are retained for our analysis (Sarkar & Pandey 2019). We choose $R_1 = 2$ Mpc and $R_2 = 10$ Mpc for the analysis presented here.

The local dimension D describes the morphology of the embedding environment. Ideally, a filamentary environment should have $D = 1$ and sheetlike environment should have $D = 2$. A homogeneous distribution in three-dimension is represented by $D = 3$. However, the filaments, sheets, clusters and voids are not idealized structures and they can have a wide variety of shapes and sizes. We assign a finite range of local dimension to each type of morphological environment as shown in Table 1. We determine the geometry of the local environment of a galaxy based on these definitions. Accordingly, the $D1$ -type galaxies reside in one dimensional nearly straight filament. A $D2$ -type galaxy is residing in a two-dimensional sheet-like structure. A $D3$ -type galaxy is embedded in a three dimensional distribution of homogeneous nature. The galaxies can also reside near the junction of different types of morphological environments. $D1.5$ and $D2.5$ can be treated as intermediate environments.

3 RESULTS AND CONCLUSIONS

We show the cumulative mean of the $u - r$ colour for the major pairs residing in sheets and filaments as a function of three-dimensional separation in the left panel of Figure 1. This shows that the major pairs with pair separation $r < 50$ kpc are on average bluer in filamentary environment compared to those residing in sheet-like environment. However, this trend only persists up to a pair separation of ~ 50 kpc. A cross over of the two curves corresponding to $D1$ and $D2$ type environments is observed at $r \sim 50$ kpc. The major pairs with pair separation $r > 50$ kpc are significantly redder in filaments compared to those located in sheets. We also analyze the SFR in major pairs residing in filaments and sheets and show the results in the right panel of Figure 1. We find that the major pairs at closer pair separation (< 50 kpc) are more star forming in filaments compared to those in sheets. We see an exactly opposite trend for the major pairs with larger pair separation (> 50 kpc). The colour and SFR are correlated properties Strateva et al. (2001); Baldry et al. (2004); Pandey (2020) and the results shown in the two panels of Figure 1 are consistent with each other. It is also interesting to note that the crossover is observed at nearly the same pair separation (~ 50 kpc) for both colour and SFR.

It is well known that the stellar mass (Kauffmann et al. 2003; Birnboim & Dekel 2003; Dekel & Birnboim 2006; Kereš et al. 2005; Gabor et al. 2010) and the available cold gas mass content (Davé, Finlator, & Oppenheimer 2012; Lilly et al. 2013; Saintonge et al. 2012; Violino et al. 2018; Thorp et al. 2022) also play a very important role in deciding the star formation in a galaxy. We test

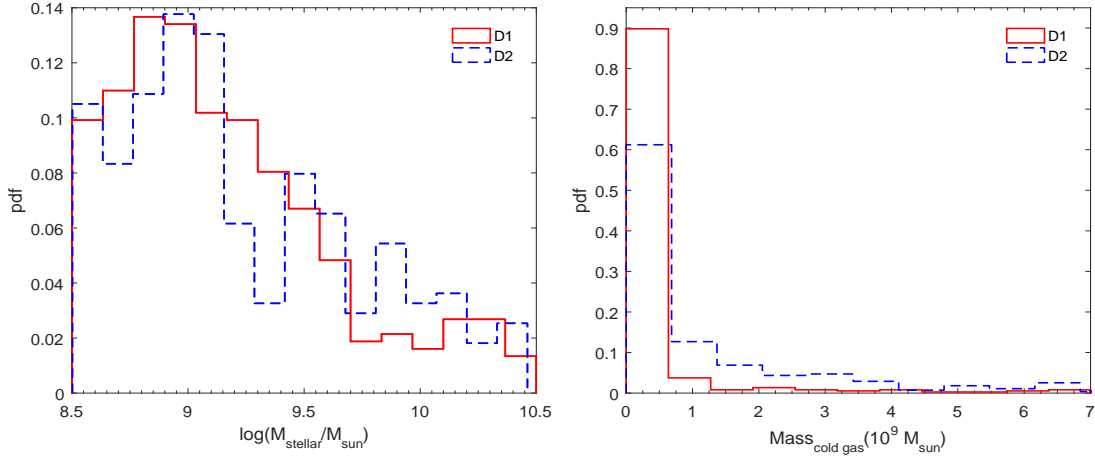


Fig. 2: The plot in the left and right panel respectively shows probability distribution function of $\log(M_{\text{stellar}}/M_{\text{sun}})$ and $Mass_{\text{coldgas}}$ of major paired galaxies residing in $D1$ and $D2$ type environments.

Major pairs	D_{KS}		$D_{KS}(\alpha)$				
	$\log(M_{\text{stellar}}/M_{\text{sun}})$	$Mass_{\text{coldgas}}$	99%	90%	80%	70%	60%
All	0.1037	0.5105	0.1292	0.0972	0.0852	0.0773	0.0712
$r < 50$ kpc	0.1032	0.3512	0.3754	0.2826	0.2478	0.2249	0.2072
$r \geq 50$ kpc	0.1055	0.5104	0.1388	0.1043	0.0915	0.0830	0.0765

Table 2: This table shows Kolmogorov-Smirnov statistic D_{KS} for comparison of $\log(M_{\text{stellar}}/M_{\text{sun}})$ and $Mass_{\text{coldgas}}$ of major pairs residing in $D1$ and $D2$ type environments. The comparison is also done for major pairs having $r < 50$ kpc and $r \geq 50$ kpc. The table also shows the critical values $D_{KS}(\alpha)$ above which null hypothesis can be rejected at different confidence levels.

if the differences occurring in $u - r$ colour and SFR of galaxies in major pairs residing in $D1$ and $D2$ type environments arise due to the differences in their stellar mass and cold gas content. We use a Kolmogorov-Smirnov (KS) test to compare the distributions of stellar mass and cold gas mass of major paired galaxies in $D1$ and $D2$ type environments. The probability distribution functions of the two properties in $D1$ and $D2$ type environments are shown in the two panels of Figure 2. We first carry out the test for the major pairs with all possible pair separations. We then conduct separate tests for the major pairs with pair separation > 50 kpc and < 50 kpc. The results for the KS test are tabulated in Table 2. The results show that null hypothesis for stellar mass and cold gas mass for all the major pairs can be rejected at 90% and 99% confidence levels respectively. This implies that the stellar mass distribution of galaxies in major pairs residing in $D1$ and $D2$ type environment are likely to be drawn from the same parent population. However, the galaxies in major pairs residing in filaments and sheets have a significantly different cold gas mass distribution. We also arrive at the same conclusions for the major pairs with $r > 50$ kpc. Interestingly, the results for the major pairs with $r < 50$ kpc suggest that the null hypothesis for stellar mass can be rejected at a very low confidence level ($< 60\%$), whereas for cold gas mass, it can be rejected at $\leq 90\%$ confidence level. Thus, stellar mass of major pair galaxies with $r < 50$ kpc in $D1$ and $D2$ type environment are highly likely to be drawn from the same parent population. This clearly shows that stellar mass and available cold gas mass of the paired galaxies are not responsible for the differences observed in their $u - r$ colour and SFR in $D1$ and $D2$ type environments at smaller pair separations ($r < 50$ kpc).

The filaments in the cosmic web are generally located at the intersection of sheets. Analysis with N-body simulations suggest that matter successively flows from voids to sheets, sheets to filaments and finally from filaments to the clusters (Aragón-Calvo, et al. 2010; Cautun, et al. 2014;

Ramachandra & Shandarin 2015; Galárraga-Espinosa, Garaldi, & Kauffmann 2022). A number of earlier studies find that the galaxy pairs are preferentially aligned with the filament axis (Tempel & Tamm 2015; Mesa et al. 2018). The alignment signal is reported to be stronger for closer pairs residing near the filament spine. The anisotropic accretion along the filaments may significantly influence the gas accretion efficiency in these aligned galaxy pairs and trigger interaction induced star formation in them. On the other hand, the major pairs with $r > 50$ kpc show a lower star formation in filaments than in sheets. The filaments are generally denser than the sheets. The $D1$ -type galaxies are embedded in high density environment as compared to the $D2$ -type galaxies (Pandey & Sarkar 2020). The galaxies in high density environments are known to be less star forming and redder compared to those residing in low density environments (Lewis et al. 2002; Gómez et al. 2003; Kauffmann et al. 2004). So naively one would expect the galaxies in filamentary environment to be less star forming and redder compared to the galaxies in sheet-like environment. We find that this is true for the galaxies in major pairs with separation larger than 50 kpc. However, the galaxies in major pairs at closer pair separation show a strikingly opposite behaviour.

The results reported in this work are very similar to the results obtained in a recent study (Das, Pandey & Sarkar 2023) of the colour and SFR of major pairs in filaments and sheets using the SDSS data. Das, Pandey & Sarkar (2023) use volume limited sample of galaxies ($M_r \leq -19$) for their analysis and find a crossover in these properties at nearly the same length scale (~ 50 kpc). It is interesting to note that we observe exactly the same trend in the EAGLE simulation data. This provides a strong theoretical support to the observational findings that large-scale structures like sheets and filaments affect galaxy interactions. This also indicates that the galaxy properties are modulated by their large-scale environment.

Finally, we conclude that the filaments play a significant role in deciding the galaxy properties and their evolution. The observed differences in the colour and SFR of major pairs in filaments and sheets can not be entirely explained by the differences in the local density and the stellar mass distributions. The galaxy pairs at smaller separations are known to trigger star formation. The filaments provide a favourable environment for such interaction. This makes the interacting galaxies bluer in filaments compared to those found in sheets.

Acknowledgements BP would like to acknowledge financial support from the SERB, DST, Government of India through the project CRG/2019/001110. BP would also like to acknowledge IUCAA, Pune for providing support through associateship programme. SS acknowledges DST, Government of India for support through a National Post Doctoral Fellowship (N-PDF).

The authors acknowledge the Virgo Consortium for making their simulation data available. The EAGLE simulations were performed using the DiRAC-2 facility at Durham, managed by the ICC, and the PRACE facility Curie based in France at TGCC, CEA, Bruyères-le-Châtel.

References

- Alonso, M. S., Tissera, P. B., Coldwell, G., Lambas, D. G., 2004, MNRAS, 352, 1081 2, 3
 Alonso, M. S., Lambas, D. G., Tissera, P., Coldwell, G., 2006, MNRAS, 367, 1029 2
 Aragón-Calvo M. A., Platen E., van de Weygaert R., Szalay A. S., 2010, ApJ, 723, 364 6
 Baldry, I. K., Glazebrook, K., Brinkmann, J., Ivezić, Ž., Lupton, R. H., Nichol, R. C. & Szalay, A. S., ApJ, 600, 681 5
 Balogh, M. L., Navarro, J. F., & Morris, S. L., 2000, ApJ, 540, 113 2
 Bharadwaj S., Sahni V., Sathyaprakash B. S., Shandarin S. F., Yess C., 2000, ApJ, 528, 21 2
 Bamford, S. P., Nichol, R. C., Baldry, I. K., et al., 2009, MNRAS, 393, 1324 2
 Barton, E. J., Arnold, J. A., Zentner, A. R., Bullock, J. S., Wechsler, R. H., 2007, ApJ, 671, 1538 2
 Barton, E. J., Geller, M. J., Kenyon, S. J., 2000, ApJ, 530, 660 2
 Bhattacharjee, S., Pandey, B., & Sarkar, S., 2020, JCAP, 2020, 039 2
 Birnboim Y., Dekel A., 2003, MNRAS, 345, 349 2, 5
 Blanton, M. R., et al., 2003, ApJ, 594, 186 2

- Bond, J. R., Kofman, L., & Pogosyan, D., 1996, *Nature*, 380, 603 2
- Cautun M., van de Weygaert R., Jones B. J. T., Frenk C. S., 2014, *MNRAS*, 441, 2923 6
- Cox, T. J., Primack, J., Jonsson, P., & Somerville, R. S., 2004, *ApJL*, 607, L87 2
- Das, A., Pandey, B & Sarkar, S., 2023, *RAA*, 02, 23 1, 2, 3, 7
- Davé R., Finlator K., Oppenheimer B. D., 2011, *MNRAS*, 416, 1354 3
- Galarraga-Espinosa, D., Aghanim, N., Langer, M., Tanimura, H., 2021, *A&A*, 649, A117 2
- Galarraga-Espinosa D., Garaldi E., Kauffmann G., 2022, arXiv, arXiv:2209.05495, Accepted in *A&A* 7
- Davé R., Finlator K., Oppenheimer B. D., 2012, *MNRAS*, 421, 98 3, 5
- Davis, M., & Geller, M.J., 1976, *ApJ*, 208, 13 2
- Dekel A., Birnboim Y., 2006, *MNRAS*, 368, 2 2, 5
- Dekel, A., Sari, R., Coverino, D., 2009, *ApJ*, 703, 785 3
- Doi, M et al., 2010, doi:10.1088/004-6256/139/4/1628, arxiv:1002.3701 4
- Dressler, A., 1980, *ApJ*, 236, 351 2
- Einasto J., Klypin A. A., Saar E., Shandarin S. F., 1984, *MNRAS*, 206, 529 2
- Einasto, J., Hüttsi, G., Einasto, M., Saar, E., Tucker, D. L., Müller, V., Heinämäki, P., & Allam, S. S. , 2003, *A&A*, 405, 425 2
- Einasto J., Joeveer M., Saar E., 1980, *MNRAS*, 193, 353 2
- Ellison, S. L., Patton, D. R., Simard, L., McConnachie, A. W., 2008, *AJ*, 135, 1877 2
- Ellison, S. L., Patton, D. R., Simard, L., McConnachie, A. W., Baldry, I. K., Mendel, J. T., 2010, *MNRAS*, 407, 1514 2
- Fall, S. M., & Efstathiou, G., 1980, *MNRAS*, 193, 189 2
- Gabor J. M., Davé R., Finlator K., Oppenheimer B. D., 2010, *MNRAS*, 407, 749 2, 5
- Gómez, P. L., Nichol, R. C., Miller, C. J., Balogh, M. L., Goto, T., Zabludoff, A. I., Romer, A. K., et al., 2003, *ApJ*, 584, 210 2, 7
- Goto, T., Yamauchi, C., Fujita, Y., Okamura, S., Seikiguchi, M., Smail, I., Bernardi, M., & Gomez, P.L., 2003, *MNRAS*, 346, 601 2
- Gregory S. A., Thompson L. A., 1978, *ApJ*, 222, 784 2
- Gunn, J. E., & Gott, J. R., 1972, *ApJ*, 176, 1 2
- Guzzo, L., Strauss, M.A., Fisher, K.B., Giovanelli, R., & Haynes, M.P., 1997, *ApJ*, 489, 37 2
- Heiderman, A., Jogee, S., Marinova, I., van Kampen, E., Barden, M., Peng, C. Y., Heymans, C. et al., 2009, *ApJ*, 705, 1433 2
- Hogg D. W., Blanton M. R., Eisenstein D. J., Gunn J. E., Schlegel D. J., Zehavi I., Bahcall N. A., et al., 2003, *ApJL*, 585, L5 2
- Joeveer M., Einasto J., 1978, *IAUS*, 79, 241 2
- Kauffmann, G., White, S. D. M., Heckman, T. M., et al., 2004, *MNRAS*, 353, 713 2, 7
- Kauffmann, G., Heckmann, T. M., White, S. D. M., Charlot, S., Tremonti, C et al., 2003, *MNRAS*, 341, 54 4, 5
- Kawata, D., & Mulchaey, J. S., 2008, *ApJL*, 672, L103 2
- Kereš D., Katz N., Weinberg D. H., Davé R., 2005, *MNRAS*, 363, 2 2, 5
- Knapen, J. H., James, P. A., 2009, *ApJ*, 698, 1437 2
- Koyama, Y., Smail, I., Kurk, J., et al., 2013, *MNRAS*, 434, 423 2
- Lambas D. G., Tissera, P. B., Alonso, M. S., Coldwell, G., 2008, *MNRAS*, 346, 1189 2
- Larson, R. B., Tinsley, B. M., & Caldwell, C. N., 1980, *ApJ*, 237, 692 2
- Lewis, I., Balogh, M., Propris, R. De., Couch, W., Bower, R., Offer, A., Bland-Hawthorn, J., et al., 2002, *MNRAS*, 334, 673 2, 7
- Lilly S. J., Carollo C. M., Pipino A., Renzini A., Peng Y., 2013, *ApJ*, 772, 119L 3, 5
- Martig M., Bournaud F., Teyssier R., Dekel A., 2009, *ApJ*, 707, 250 2
- Masters K. L., Mosleh M., Romer A. K., Nichol R. C., Bamford S. P., Schawinski K., Lintott C. J., et al., 2010, *MNRAS*, 405, 783 2
- McAlpine, S., Helly, J. C., Schaller, M., Trayford, J. W. et al., 2016, *A&C*, 72, 15 3
- Mesa V., Duplancic F., Alonso S., Muñoz Jofré M. R., Coldwell G., Lambas D. G., 2018, *A&A*, 619, A24 3, 7

- Moore, B., Katz, N., Lake, G., Dressler, A., & Oemler, A., 1996, *Nature*, 379, 613 2
- Moore, B., Lake, G., & Katz, N., 1998, *ApJ*, 495, 139 2
- Mouhcine, M., Baldry, I. K., & Bamford, S. P., 2007, *MNRAS*, 382, 801 2
- Murray, N., Quataert, E., & Thompson, T. A., 2005, *ApJ*, 618, 569 2
- Nikolic, B., Cullen, H., Alexander, P., 2004, *MNRAS*, 355, 874 2
- Oemler, A., 1974, *ApJ*, 194, 1 2
- Pandey B., & Bharadwaj S., 2005, *MNRAS*, 357, 1068 2
- Pandey, B., & Bharadwaj, S., 2006, *MNRAS*, 372, 827 2
- Pandey, B., & Bharadwaj, S., 2008, *MNRAS*, 387, 767 2
- Pandey, B., & Sarkar, S., 2017, *MNRAS*, 467, L6 2
- Pandey, B., & Sarkar, S., 2020, *MNRAS*, 498, 6069 2, 7
- Pandey B., 2020, *MNRAS*, 499, L31 5
- Park C., Choi Y.-Y., Vogeley M. S., Gott J. R., Blanton M. R., SDSS Collaboration, 2007, *ApJ*, 658, 898 2
- Patton, D. R. & Atfield, J. E., 2008, *ApJ*, 685, 235
- Peng Y.-jie., Renzini A., 2020, *MNRAS*, 491, L51 2
- Planck Collaboration et al., 2014, *A&A*, 571, A1 3
- Porter, S. C., Raychaudhury, S., Pimblet, K. A., Drinkwater, M. J., 2008, *MNRAS*, 388, 1152 2
- Ramachandra N. S., Shandarin S. F., 2015, *MNRAS*, 452, 1643 7
- Rees, M. J. & Ostriker, J. P., 1977, *MNRAS*, 179, 541 2
- Robaina, A. R., Bell, E. F., Skelton, R. E., Mcintosh, D. H., Somerville, R. S., Zheng, X., Rix, H.-W. et al., 2009, *ApJ*, 704, 324 2
- Saintonge A., Tacconi L. J., Fabello S., Wang J., Catinella B., Genzel R., Graciá-Carpio J., et al., 2012, *ApJ*, 758, 73 5
- Sarkar, P. & Bharadwaj, S., 2009, *MNRAS*, 394, L66 3, 4
- Sarkar, S., & Pandey, B., 2019, *MNRAS*, 485, 4743 5
- Sarkar, S., & Pandey, B., 2020, *MNRAS*, 497, 4077 2
- Silk, J., 1977 *ApJ*, 211, 638 2
- Somerville, R. S., & Primack, J. R., 1999, *MNRAS*, 310, 1087 2
- Springel, V., Di Matteo, T., & Hernquist, L., 2005, *MNRAS*, 361, 776 2
- Strateva I., Ivezić Ž., Knapp G. R., Narayanan V. K., Strauss M. A., Gunn J. E., Lupton R. H., et al., 2001, *AJ*, 122, 1861 5
- Tempel E., Tamm A., 2015, *A&A*, 576, L5 3, 7
- Thorp M. D., Ellison S. L., Pan H.-A., Lin L., Patton D. R., Bluck A. F. L., Walters D., et al., 2022, *MNRAS*, 516, 1462 5
- Trayford, J. W et al., 2015, *MNRAS*, 452, 2879 4
- Tuominen T., Nevalainen J., Tempel E., Kuutma T., Wijers N., Schaye J., Heinämäki P., et al., 2021, *A&A*, 646, A156 2
- Violino G., Ellison S. L., Sargent M., Coppin K. E. K., Scudder J. M., Mendel T. J., Saintonge A., 2018, *MNRAS*, 476, 2591 5
- White, S. D. M., & Rees, M. J., 1978 *MNRAS*, 183, 341 2
- Woods, D. F., Geller, M. J., 2007, *AJ*, 134, 527 2
- Woods, D. F., Geller, M. J., Barton, E. J., 2006, *AJ*, 132, 197 2
- Woods, D. F., Geller, M. J., Kurtz, M. J., Westra, E., Fabricant, D. G., Dell'Antonio, I., 2010, *AJ*, 139, 1857 2
- Zehavi, I., et al. 2002, *ApJ*, 571, 172 2
- Zeldovich I. B., Shandarin S. F., 1982, *PAZh*, 8, 131 2